Fatigue crack micromechanisms in a Cu-Zn-Al shape memory alloy with pseudo-elastic behavior

Vittorio Di Cocco, Francesco Iacoviello
Università di Cassino e del Lazio Meridionale, DICeM, Cassino (FR), Italy
v.dicocco@unicas.it, iacoviello@unicas.it

Stefano Natali, Andrea Brotzu
Università di Roma "Sapienza", D.I.C.M.A., via Eudossiana 18, 00184 Roma
stefano.natali@uniroma1.it, andrea.brotzu@uniroma1.it

ABSTRACT. Shape memory property characterizes the behavior of many Ti based and Cu based alloys (SMAs). In Cu-Zn-Al SMAs, the original shape recovering is due to a bcc phase that is stable at high temperature. After an appropriate cooling process, this phase (β-phase or austenitic phase) transforms reversibly into a B2 structure (transition phase) and, after a further cooling process or a plastic deformation, it transforms into a DO_3 phase (martensitic phase). In β-Cu-Zn-Al SMAs, the martensitic transformation due to plastic deformation is not stable at room temperature: a high temperature "austenitization" process followed by a high speed cooling process allow to obtain a martensitic phase with a higher stability.
In this work, a Cu-Zn-Al SMA in "as cast" conditions has been microstructurally and metallographically characterized by means of X-Ray diffraction and Light Optical Microscope (LOM) observations. Fatigue crack propagation resistance and damaging micromechanisms have been investigated corresponding to three different load ratios (R=0.10, 0.50 and 0.75).

KEYWORDS. Zn-Cu-Al alloy; Pseudoelastic behaviour; Fatigue Crack Micromechanisms; Microstructure.

INTRODUCTION

Shape memory property characterizes the behavior of many Ti based and Cu based alloys (SMAs). This property is due to a metallurgical phenomenon, which allows to change the lattice structure without boundaries changing as a reversible transition. Equiatomic NiTi alloys and Cu-Zn-Al alloys are among the most industrially used SMAs: they are characterized by two different mechanical behaviours in terms of shape recovering:

- A shape memory effect (SME). This is obtained when the recovery of the initial shape takes place only after heating over a critical temperature, with a consequent crystallographic structure transition;
- A pseudoelastic effect (PE). This is obtained when the critical temperature is lower than environmental temperature. In this case, the recovery of the initial shape takes place only after unloading.

In the last years [1], many alloys characterized by memory property have been studied. Often the composition was characterized by the presence of rare metals and poor mechanical properties and effects that did not allow an industrial development on a large scale.
Cu-Zn-Al alloys are characterized by good shape memory properties due to a β-phase (bcc disordered structure, sometimes named austenite) that is stable at high temperature. A cooling process induces the transformation of the β-phase into a B2 structure (sometimes named as martensite) and a further cooling implies the transformation of the B2 phase into a DO_3 phase (martensitic phase). Martensitic phases can be either thermally-induced or stress-induced.
In recent years, improved mechanical properties of many SMAs allowed their application in many specific industrial applications [2-5].
Cu-based shape memory alloys are characterized by the precipitation of many different intermetallic phases and this can negatively affects their mechanical properties. Cu based alloys with low Al content are characterized by the precipitation of α-phase: this implies a strong degradation of shape recovery [6]. Anyway, Cu-Zn-Al SMAs characterized by aluminum contents less than 5% are characterized by a good cold workability, with a cost that is lower than traditional NiTi SMAs.
In this work, a Cu-Zn-Al SMA in "as cast" conditions has been microstructurally and metallographically characterized by means of X-Ray diffraction and Light Optical Microscope (LOM) observations. The investigated alloy is characterized by the stress-strain curve shown in Fig. 1 [7].
Fatigue crack propagation resistance and crack propagation micromechanisms have been investigated considering three different load ratios (R = 0.10, 0.50 and 0.75).

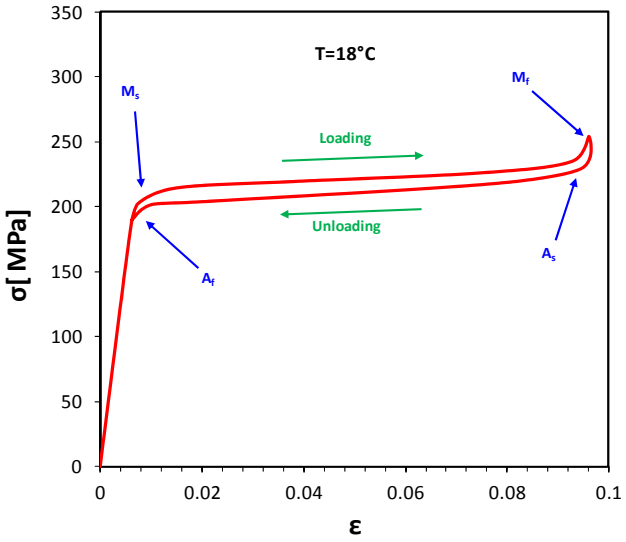

Figure 1: Cu-Zn-Al SMA stress-strain curve with hysteresis [7].

MATERIAL AND METHODS

The investigated Cu-Zn-Al SMA (chemical composition is shown in Tab. 1) was obtained by means of an atmosphere controlled furnace by using nitrogen gas, in order to reduce the presence of oxides and other precipitates (e.g, non-metallic inclusions are often due to oxidation process of evaporated Zn at high temperatures). Obtained castings were characterized by a pseudo-elastic behavior. Mini ingots were obtained by means of centrifugal furnace and casted into mold with a CT specimen shape. Solidification and cooling process were performed in lab conditions.

Cu	Zn	Al	Other
72.20	21.71	5.77	0.32

Table 1: Chemical composition of Cu-Zn-Al investigated alloy.

Alloy microstructure was investigated following the procedure described in ASTM E407-07 [8]. In order to evaluate the differences of diffraction spectra due to phases transformation, X-ray diffraction test were performed using minitensile specimens [9] considering both loaded and unloaded conditions. X-ray light was characterized by wave length of 1.53995 Å (Cu filament) and the analysis software PowderCell 2.3 [10] was used.
Finally, CT specimens were obtained using the casted ingots according to ASTM E 647 [11]. Specimens lateral surfaces were metallographically prepared and chemically etched according to ASTM E407-07 [8]. This procedure allowed the specimens lateral surfaces observations by means of a light optical microscope (LOM). Fatigue crack propagation tests were performed by means of an hydraulic testing machine according to ASTM E 647 standard [11].
Fatigue crack propagation test were performed according the following conditions:

- Stress ratio R = P_{min}/P_{max}=0.10, 0.50, 0.75:
- ΔP = constant
- Sinusoidal waveform
- Loading frequency=30Hz
- Lab conditions

Fracture surfaces were analyzed by means of a Scanning Electron Microscope (SEM) in order to evaluate the main crack micromechanisms corresponding to the different applied ΔK values.

RESULTS AND DISCUSSION

Microstructural analysis and X-ray diffraction results

LOM observations show a grain diameter mean value of about 600μm. Microstructure is not completely homogeneous and grains are characterized by a needle like morphology as shown in Fig. 2a and b.

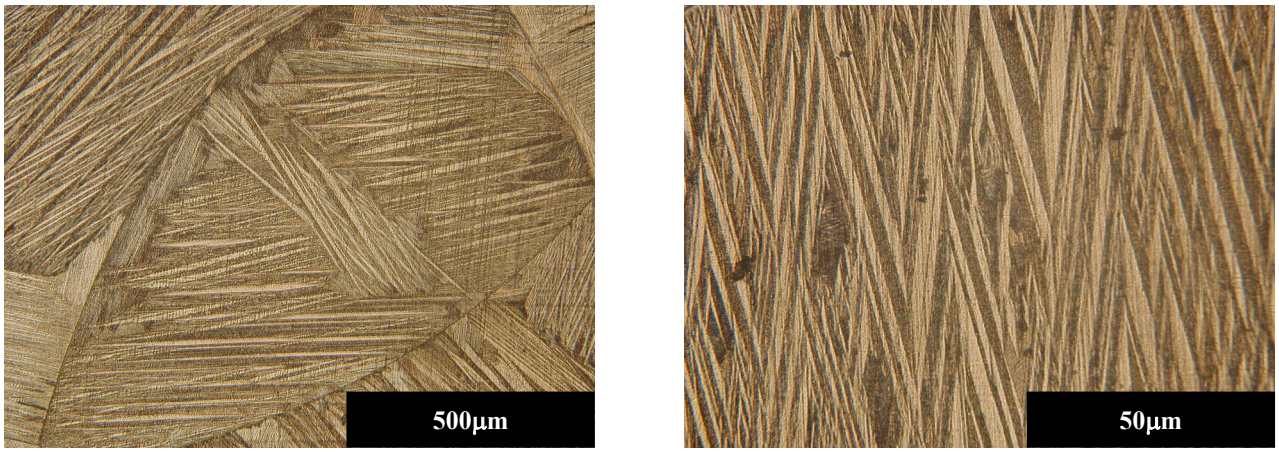

a) b)

Figure 2: Etched surface of investigated material: a) grain, b) bulk needles.

Needles structure covers the complete diameter of grains. No subgrains are observed.
X-ray analyses are shown in Fig. 3, where, in unloaded condition, four main peaks at 2θ=79.79, 43.46, 41.73 and 70.23° are evident. Under loaded conditions, they sharply reduce and new peaks grow at 2θ=68.86 and at 2θ of 41.73°. The observed spectra are very close to spectra observed by authors in a previous work [3]. Difference between "unloaded" and "loaded" conditions are due to the microstructure modification due to the presence of induced martensite.

Fatigue crack propagation results

Fatigue crack propagation results are shown in Fig. 4.
Considering R = 0.10 (Fig. 4a), five different stages can be observed [3]. It is worth to note the presence of a plateau in the stage III (with a crack growth rate of about 4 10^{-8} m/cycle). Stages I and II approximately correspond to the threshold stage and to a sort of Paris stage with a high "m" value, whereas stages IV and V correspond to a sort of Paris stage (but

with a lower slope if compared to stage II) and to the final rupture stage, respectively. For R = 0.50, stage II observed for R = 0.10 seems to "disappear" and a plateau is still evident for a crack growth rate of about 10^{-8} m/cycle (stage II, Fig 4b). Finally, for R = 0.75, the classic three crack propagation stages are obtained and no "plateau" with constant crack growth rate is evident.

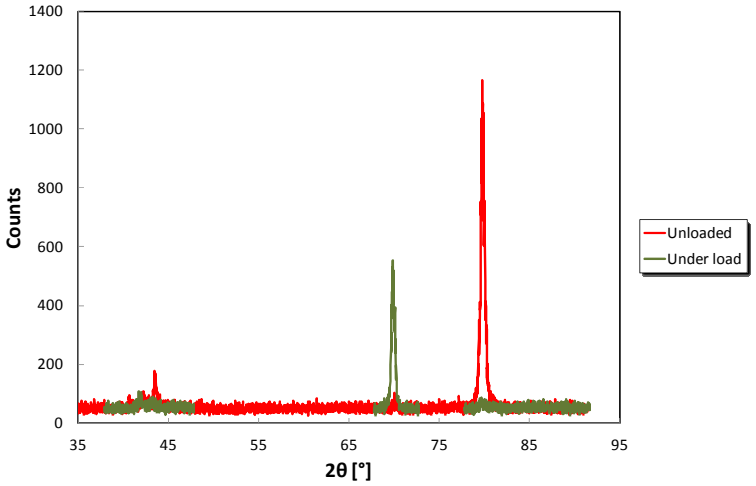

Figure 3: Investigated Cu-Zn-Al SMA spectra in unloaded and loaded conditions.

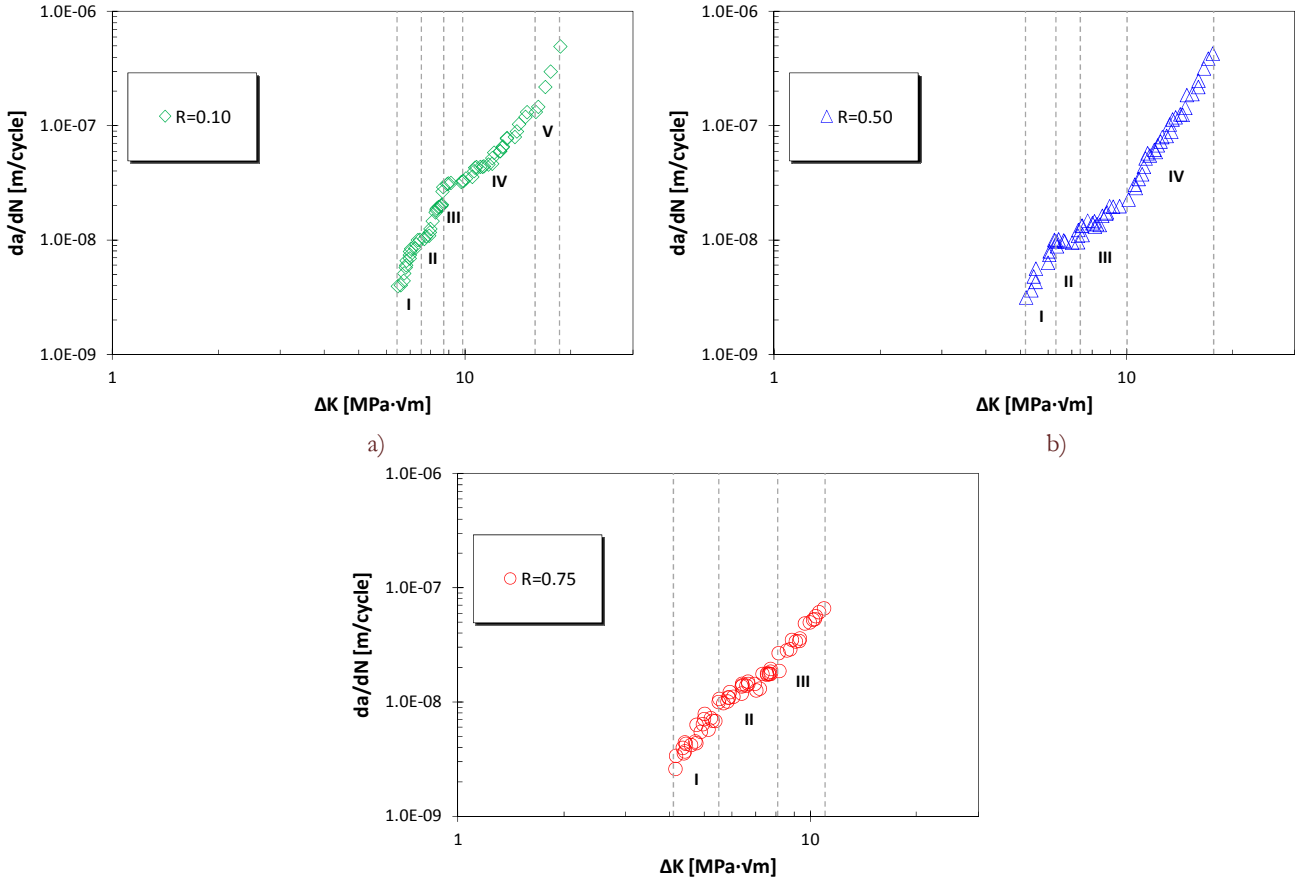

a) b) c)

Figure 4: Fatigue crack propagation da/dN-ΔK curves: a) R=0.10, b) R=0.50 and c) R=0.75.

Comparing the crack propagation results for R = 0.10 and R = 0.50 (Fig. 5), the influence of the stress ratio R on the constant crack growth rate stage is evident. The decrease of the crack growth rate values correspond to a decrease of the ΔK range where this phenomenon is evident.

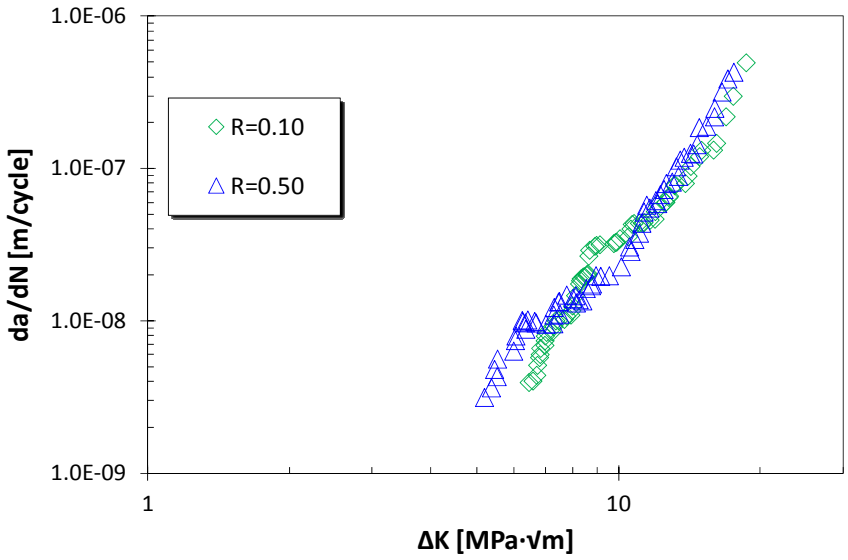

Figure 5: Comparing fatigue crack propagation behavior for R=0.10 and R=0.50 conditions.

The influence of the microstructure modification on fatigue crack propagation micromechanisms is shown in Fig. 6, where fracture surfaces obtained for R=0.10 and R=0.50 are compared (ΔK=10 MPa√m). Corresponding to this ΔK, specimen tested at R=0.10 is in the stage 3: fatigue crack mainly propagates intergranularly, with a "striation-like" morphology, probably due to the need-like microstructure (compare Fig. 6 with Fig.2). For R=0.50 the intergranular morphology is less evident (Fig. 6b), with evident fatigue striations. Difference between "striation-like" morphology and "fatigue striation" can be determined considering the striation spacing (for R = 0.10, "striation spacing" is analogous to the needles thickness).

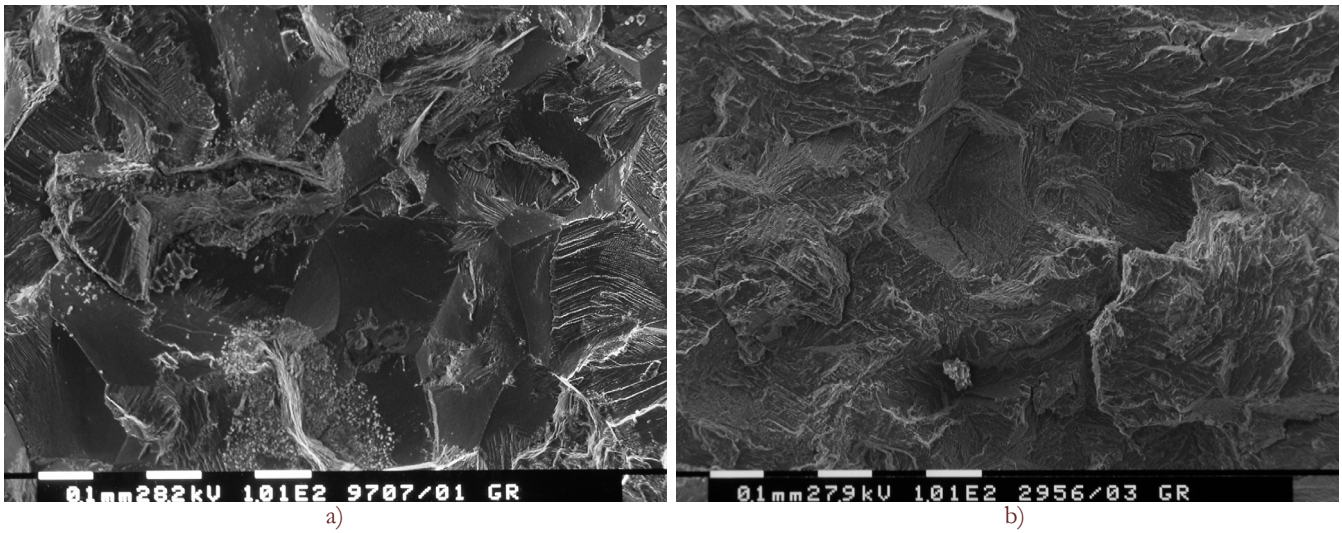

a) b)

Figure 6: Fracture surface SEM analyses: a) Stage 3 at ΔK=10 MPa√m in R=0.10 condition [3], b) Stage 3 at ΔK=10 MPa√m in the R=0.50 condition.

Considering higher ΔK values (e.g., ΔK=12 MPa√m, Fig. 7), striations are more evident and the higher R value (0.75) corresponds to a more fragile morphology, with evident intergranular secondary cracks and cleavage.

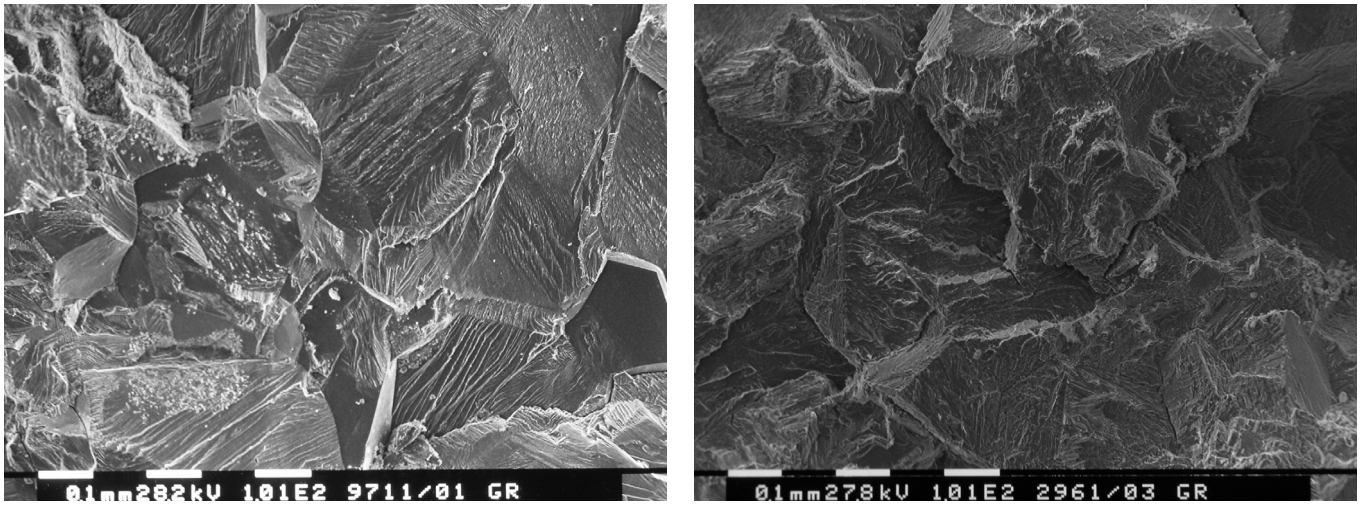

a) b) c)

Figure 7: Fracture surface SEM analyses in martensitic phase: a) R=0.10, b) R=0.50 and c) R=0.75.

According to the authors, different morphological and mechanical parameters should be taken into account in order to define the damaging micromechanisms. The main parameters are:

- Alloy microstructure: large austenitic grains (diameters mean value equal to 600 μm) and needles-like substructure;
- Shape memory micromechanisms with the presence of a hysteresis during the loading-unloading process.

Considering the peculiar behavior of the investigated alloy (Fig. 1), classic relationships [12] can't be applied to quantify the reversed plastic zone (rpz) radius. Anyway, this radius increases with the increase of the applied ΔK and, considering that the microstructure is characterized by large grains and that these grains transform from austenite to martensite due to the applied local stress, damaging micromechanisms change with the applied ΔK, becoming more and more fragile (intergranular secondary cracks + cleavage) when more critical loading conditions are applied (high R and ΔK values). These more critical conditions imply a large martensitic transformation with a reduced importance of the M ↔ A hysteresis. Further investigations are still necessary.

CONCLUSIONS

In this work, the fatigue crack propagation in a Cu-Zn-Al SMA was investigated. Fatigue crack propagation tests were performed considering three different stress ratios (R=0.10, 0.50 and 0.75, respectively).
According to the observed stress induced microstructural transformations and considering that the investigated alloy

is characterized by large grains (about 600 μm), considering the fatigue crack propagation results and the SEM fracture surface analysis, the following conclusions can be summarized:

- The investigated SMA is characterized by a stress-induced transformation.
- Investigated SMA fatigue crack propagation resistance is strongly affected by the microstructure peculiarities (e.g., grain size) and by the stress induced microstructural transformations. The presence of a plateau in the da/dN-ΔK results (for the lower R values) is probably related to transition conditions (crack tip plastic zone that become larger than grains size + increase of the importance of the microstructure transformation);
- Martensitic transformation becomes more and more important with the increase of the R and/or ΔK values. Corresponding to the more critical conditions (highest R and ΔK values) higher crack growth rates correspond to an increase of the cleavage and of intergranular secondary cracks on the fracture surface.

REFERENCES

[1] Suzuki, T., Kojima, R., Fujii, Y., Nagasawa, A.,. Reverse transformation behaviour of the stabilized martensite in Cu10at%Zn19at%Al alloy. Acta Metall. 37 (1989) 163–168.
[2] Di Cocco, V., Iacoviello, F., Natali, S., Two Cycles deformation effects on NiTi pseudoelastic alloy microstructure, In: IGF Workshop proceedings, Forni di Sopra, Italy, (2012) 62-67.
[3] Di Cocco, V., Iacoviello, F., Natali, S., Volpe, V., Fatigue crack behavior on a Cu-Zn-Al SMA, Frattura ed Integrità Strutturale, 30 (2014) 454-461; DOI: 10.3221/IGF-ESIS.30.55
[4] Ma, J., Karaman, I., Noebe, R.D., High Temperature Shape Memory Alloys. International Materials Reviews, 55(5) (2010) 257-315.
[5] Otsuka, K., Ren, X., Physical metallurgy of Ti–Ni-based shape memory alloys. Progress in Materials Science, 50 (2005) 511-678.
[6] Asanovic, V., Delijic, K., Jaukovic, N., A study of transformation of β-phase in Cu-Zn –Al shape memory alloys. Scripta Materialia, 58 (2008) 599-601.
[7] Volpe, V., Realizzazione e caratterizzazione di leghe a memoria di forma a base rame, Ph.D. thesis, University of Rome "Sapienza", (2013).
[8] ASTM E407-07, Standard Practice for Microetching Metals and Alloys, ASTM International.
[9] Di Cocco, V., Iacoviello, F., Tomassi, L., Rossi, A., Natali, S., Volpe, V., Crack path in a Cu-Zn-Al PE alloy under uniaxial load, Acta Fracturae, (2013) 255-261.
[10] PowderCell 2.3 handbook: Pulverdiffraktogrammeaus Einkristalldaten und Anpassungexperimenteller Beugungsaufnahmen. Available at http://www.bam.de/de/service/publikationen/powder_cell.htm.
[11] ASTM E 647-08, "Standard Test Method for Measurement of Fatigue Crack Growth Rates", ASTM International.
[12] Maletta, C., Furgiuele, F., Fracture control parameters for NiTi based shape memory alloys, International Journal of Solids and Structures, 48 (2011) 1658–1664.